

Fig. 4-32 I_D/I_G ratios of the as-deposited (a) Co-, (b) Ni-, and (c) Fe-assisted carbon nanostructures under different deposition times.

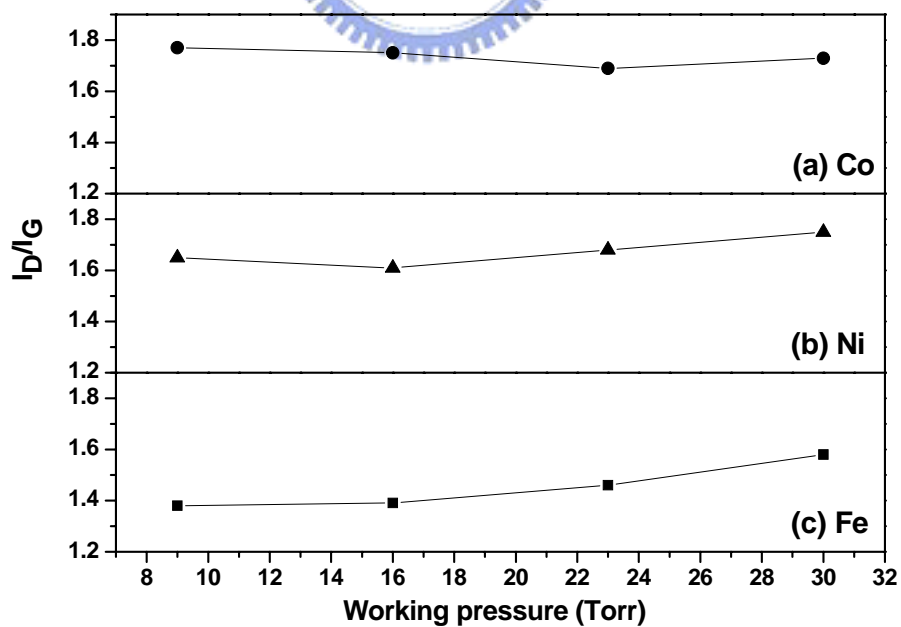


Fig. 4-33 I_D/I_G ratios of the as-deposited (a) Co-, (b) Ni-, and (c) Fe-assisted carbon nanostructures under different working pressures.

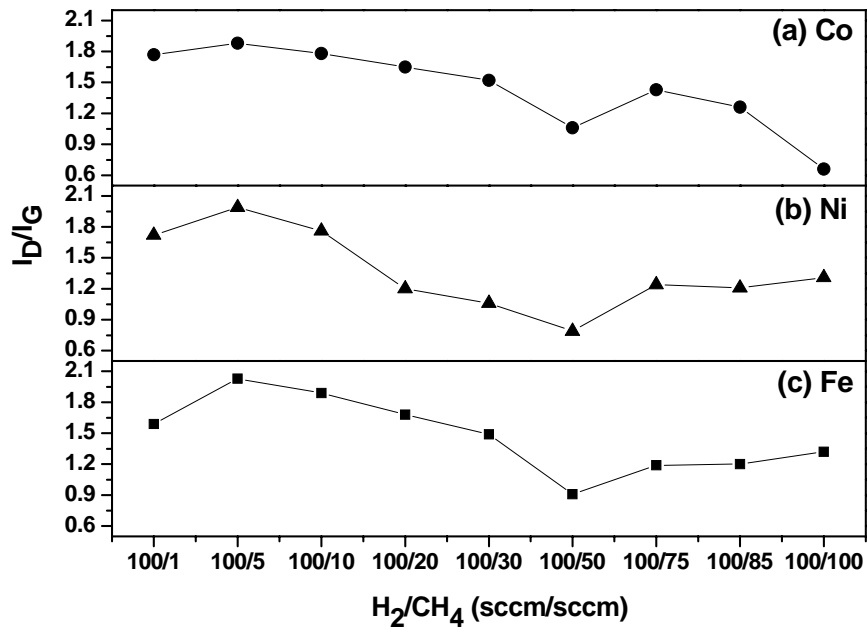


Fig. 4-34 I_D/I_G ratios of the as-deposited (a) Co-, (b) Ni-, and (c) Fe-assisted carbon nanostructures under different H_2/CH_4 flow ratios.

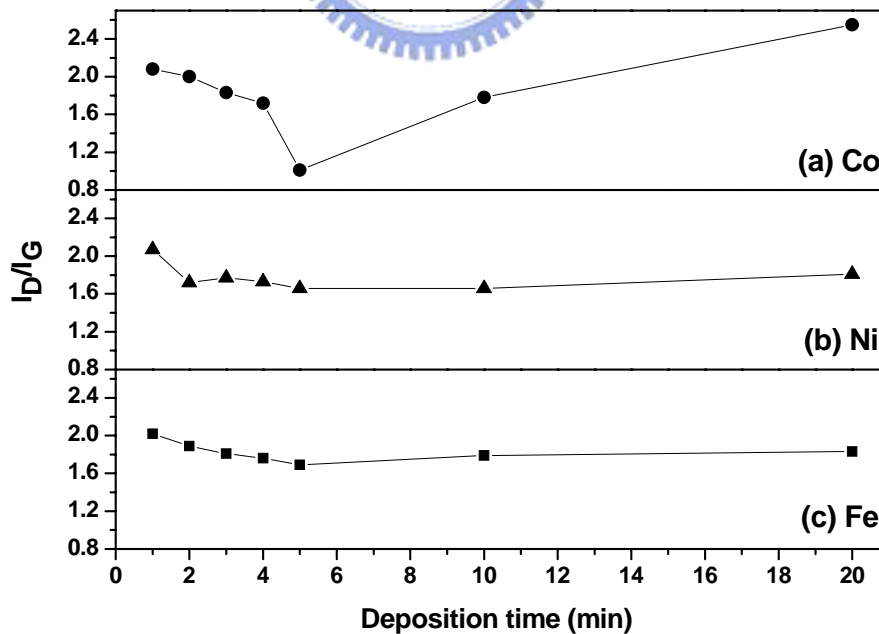


Fig. 4-35 I_D/I_G ratios of the as-deposited (a) Co-, (b) Ni-, and (c) Fe-assisted carbon nanostructures with $H_2/CH_4=0/1$ (sccm/sccm) under different deposition times.

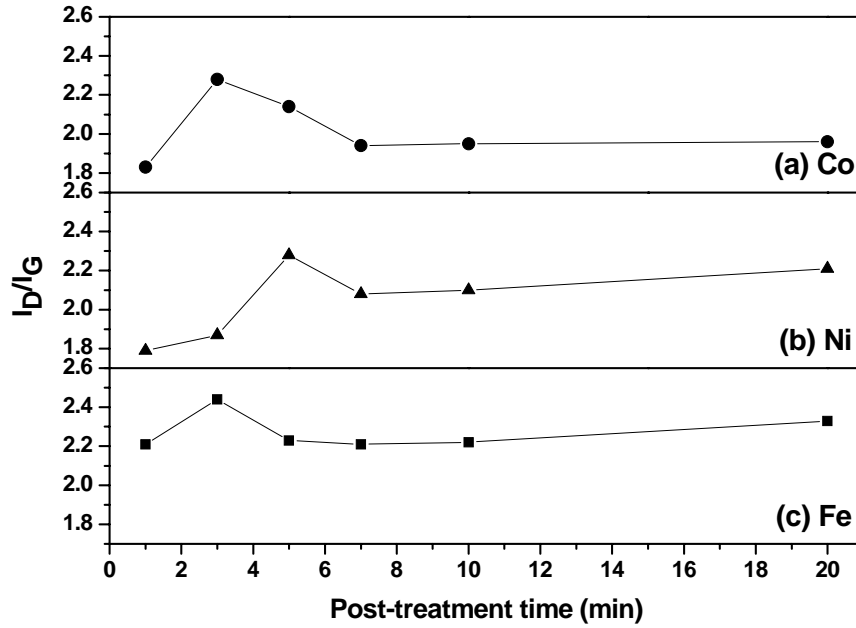


Fig. 4-36 I_D/I_G ratios of the as-deposited nanostructures for Specimens A5, B5, and C5 after different H-plasma post-treatment times.

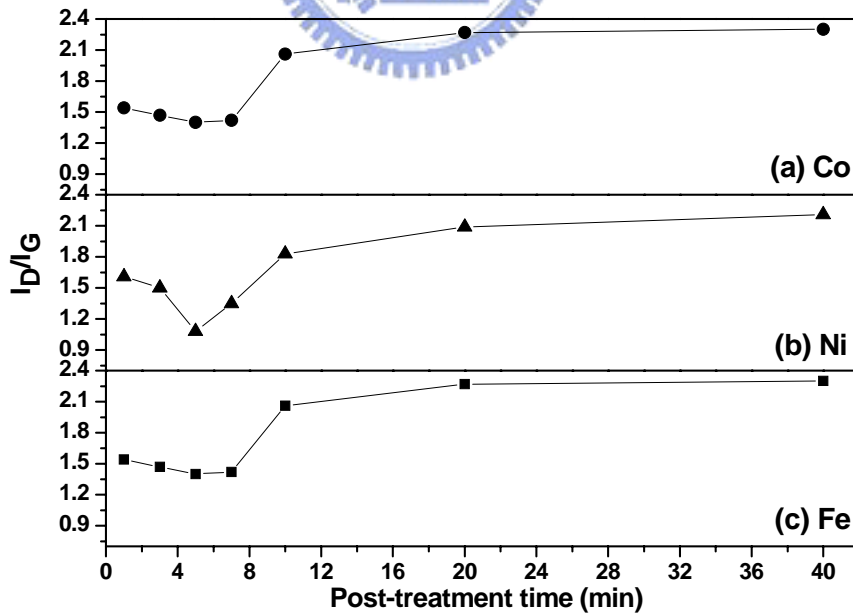


Fig. 4-37 I_D/I_G ratios of the as-deposited nanostructures for Specimens H4, I4, and J4 after different H-plasma post-treatment times.

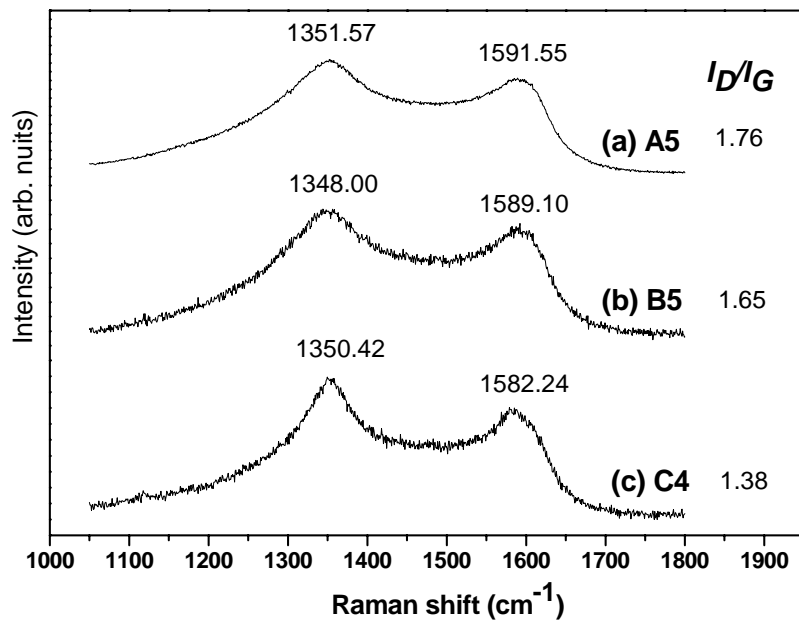


Fig. 4-38 Raman spectra of the as-deposited carbon nanocone structures for Specimens A5 (a), B5 (b), and C5 (c).

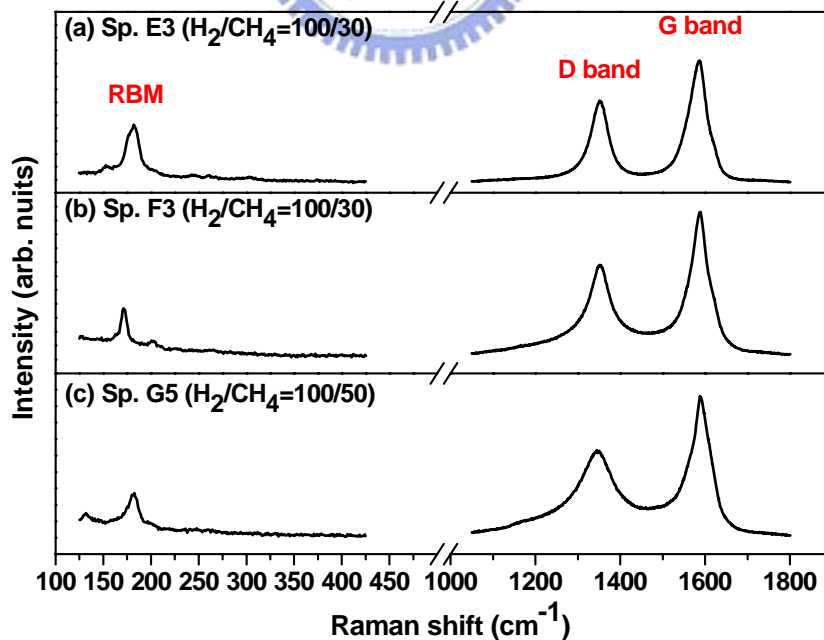


Fig.4-39 Raman spectra of the as-deposited carbon nanostructures for Specimens (a) E3, (b) F3, and (c) G5.

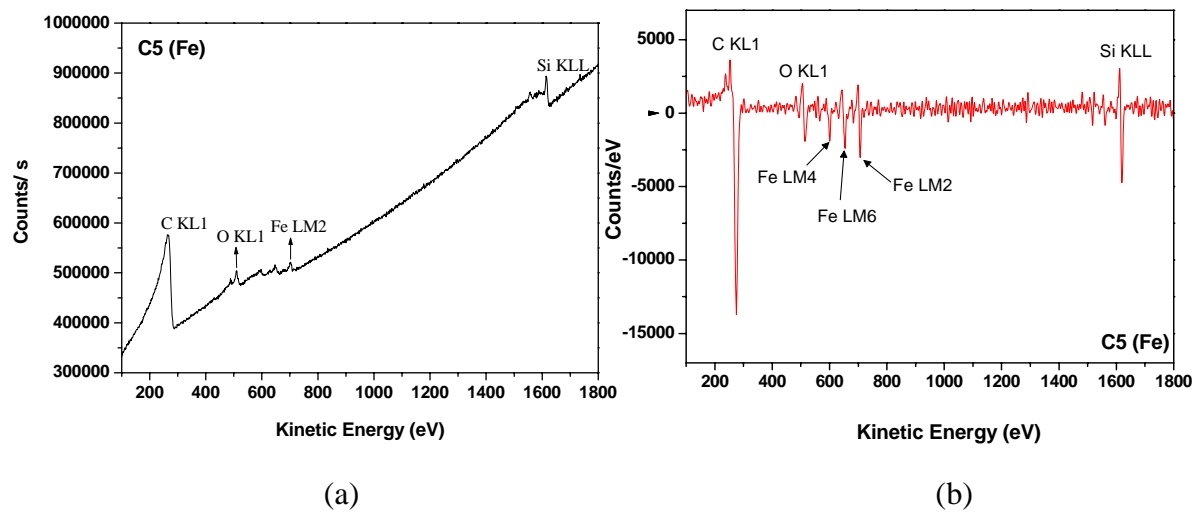


Fig.4-40 AES spectra of the as-deposited Fe-assisted carbon nanocone structures for Specimen C5. (a) the integral figure of AES survey, and (b) the differential figure of AES survey.

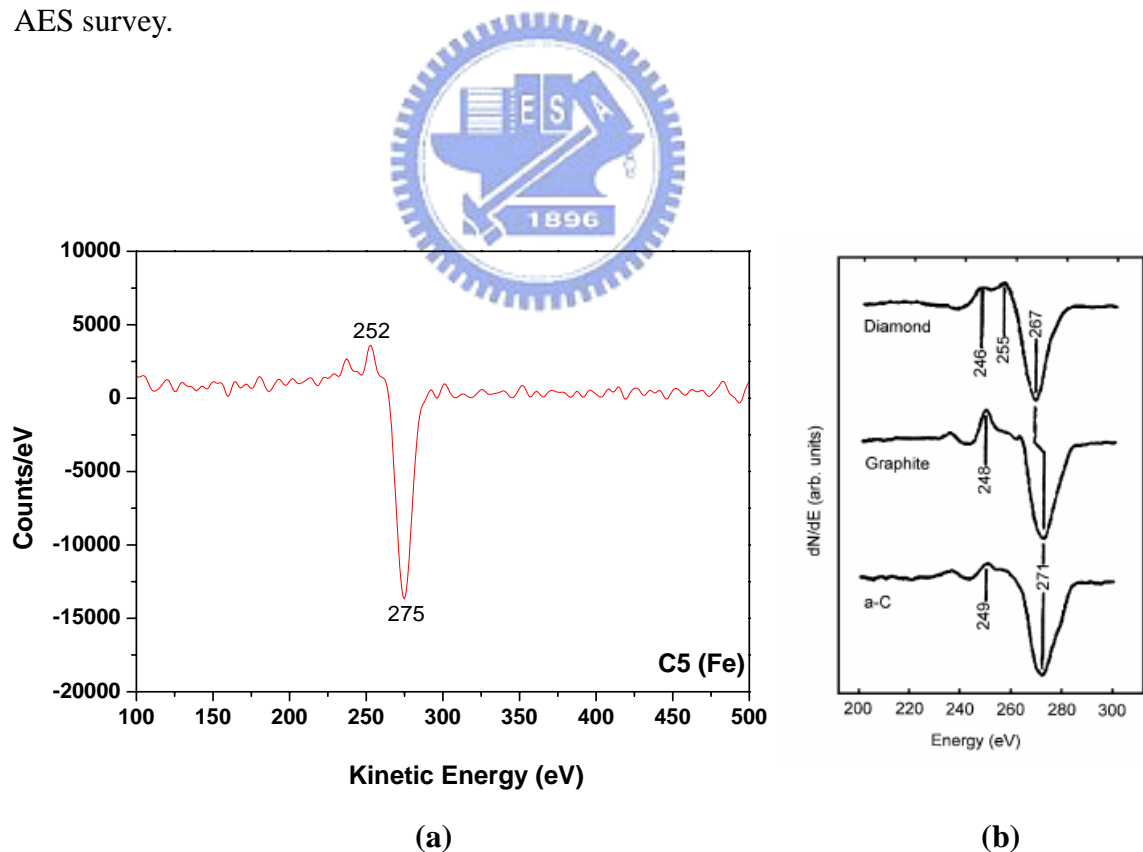


Fig.4-41 The AES spectra are corresponding to the Figs.4-40 at selective segment. (a) AES spectrum of carbon, and (b) reference spectrum of carbon [Lin-01-126].

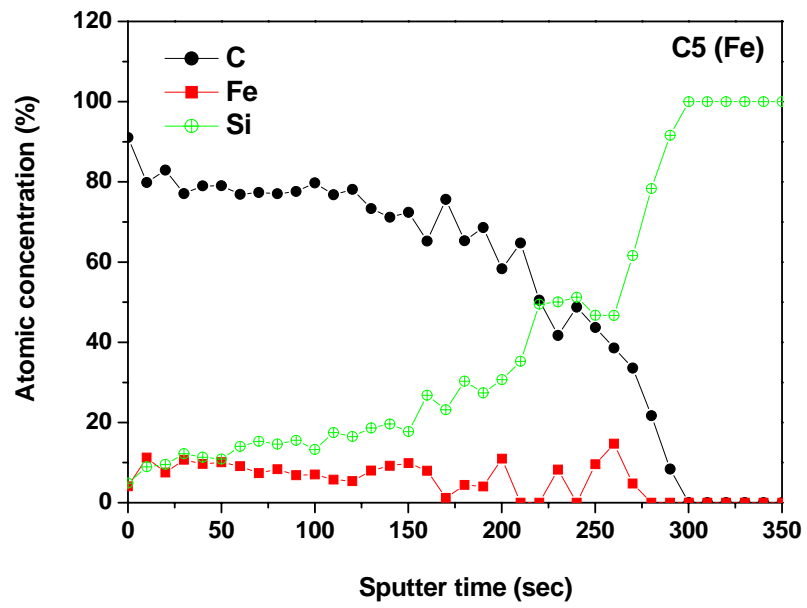


Fig.4-42 The AES depth profile analysis of Specimen C5.

